CrossMark

ORIGINAL ARTICLE

Evgeniy Yu. Vitokhin · Elena A. Ivanova

Dispersion relations for the hyperbolic thermal conductivity, thermoelasticity and thermoviscoelasticity

Abstract The Maxwell–Cattaneo heat conduction theory, the Lord–Shulman theory of thermoelasticity and a hyperbolic theory of thermoviscoelasticity are studied. The dispersion relations are analyzed in the case when a solution is represented in the form of an exponential function decreasing in time. Simple formulas that quite accurately approximate the dispersion curves are obtained. Based on the results of analysis of the dispersion relations, an experimental method of determination of the heat flux relaxation time is suggested.

1 Introduction

A study of wave heat conduction models is important for the development of modern technologies which are applied to manufacture various micro- and nano-electromechanical systems (MEMS/NEMS). This is due to the fact that using the classical heat conduction equation we cannot achieve a good agreement with experimental data when we model non-stationary thermal processes caused by nano-sized internal heat sources or by short-time impulse excitations [1,2]. In order to model such processes, more complicated models of heat conduction were suggested. We refer to models with finite propagation velocity of thermal disturbances [2–5], models with thermal memory that take into account a heating history [6], models taking into account the finite heat flux delay time and the finite temperature gradient delay time [4,7]. A detailed overview of the heat conduction models can be found in [2].

The Maxwell–Cattaneo model is one of the most known models of non-Fourier heat conduction. This model allows us to achieve more reliable results in the problems of metal heating by means of shot laser impulses [8], in the case of a heat source motion with a high velocity [7], and in the case of a rapid motion of a phase boundary [9]. The derivation of the Maxwell–Cattaneo heat conduction equation is based on the heat conduction law suggested independently by three scientists, namely Cattaneo [10], Vernotte [11] and Lykov [12]. This law has the form

$$\tau \dot{\mathbf{h}} + \mathbf{h} = -\lambda \nabla T, \tag{1}$$

E. Yu. Vitokhin (✉) · E. A. Ivanova
Department of Theoretical Mechanics, Peter the Great Saint-Petersburg Polytechnic University, Polytechnicheskaya, 29,
St. Petersburg, Russia 195251
E-mail: evitokhin@yandex.ru

E. A. Ivanova
Institute for Problems in Mechanical Engineering of Russian Academy of Sciences, Bolshoy pr. V.O., 61, St. Petersburg,
Russia 199178
E-mail: elenaivanova239@gmail.com

where $\mathbf{h}$ is the heat flux vector, dot denotes the time derivative, ∇ is the nabla operator, T is temperature, λ is the heat conduction coefficient, τ is the heat flux relaxation time (a constant). The Cattaneo–Vernotte law is the generalization of the Fourier law. The presence of the finite relaxation time τ in Eq. (1) means that the heat flux does not appear (disappear) simultaneously with the appearance (disappearance) of temperature gradient. The derivation of the Maxwell–Cattaneo equation is carried out as follows. Let us consider a heat-conducting rigid body. The energy balance equation is formulated as

$$\rho \dot{U} = -\nabla \cdot \mathbf{h} + \rho q, \tag{2}$$

where ρ is the volume density of mass, U is the mass density of the internal energy, q is the rate of heat supply per unit mass.

It is known that the linear heat conduction equation can be used if the deviations of temperature from its reference value T_* (the value at which all thermodynamic parameters are measured) are less than 10 K. That is why, the mass density of internal energy can be represented as follows:

$$U = c_v \tilde{T}, \qquad \tilde{T} = T - T^*, \tag{3}$$

where c_v is the specific heat at constant volume. Next, let us substitute (3), into Eq. (2). Then, taking into account the Cattaneo–Vernotte law (1), we obtain the Maxwell–Cattaneo heat conduction equation

$$\lambda \Delta \tilde{T} - \rho c_v \left(\dot{\tilde{T}} + \tau \ddot{\tilde{T}} \right) + \rho \left(q + \tau \dot{q} \right) = 0, \tag{4}$$

where Δ is the Laplace operator. Equation (4) is the hyperbolic type equation. It combines properties of both the classical heat conduction equation and the wave equation. As seen from Eq. (4), the thermal wave propagation velocity depends on the heat flux relaxation time τ. An analytical solution of Eq. (4) in the case of laser action can be found, e.g., in [13].

In 1944, Peshkov detected the thermal waves by experiment based on using the superfluid helium at low temperature near the absolute zero [14]. He called them "the second sound" because the propagation velocity of these waves was near to the propagation velocity of acoustic waves. At the present time, methods of measurement of temperature and parameters characterizing the thermodynamic properties of materials are rapidly developed. A laser thermometry technique is one of the modern methods of temperature measurement [15–17]. It consists in remote measuring a temperature-dependent parameter by means of the probing light beam and calculating the temperature by using the known temperature dependence of the measured parameter. Five noncontact and nondestructive methods of temperature measurement are discussed in [18]. They are the optical heating and electrical sensing technique, the transient electro-thermal technique, the transient photo-electro-thermal technique, the pulsed laser-assisted thermal relaxation technique, and the steady-state electro-Raman-thermal technique. An experimental determination of the heat flux relaxation time τ based on the method of thermodynamic lattices is discussed in [19–21]. A brief outline of the method is as follows: a thermodynamic lattice of a given period is formed in a material (to be exact, a redundant temperature distributed as cosine, the period of which is equal to the lattice period, is generated in the direction of the lattice vector), and after cessation of the external influence the relaxation process is registered by a laser.

In spite of a rapid development of measurement technique, as asserted in [22, p. 75], at present there are no direct methods of measurement of the heat flux relaxation time. In addition, we note that values of τ for various substances, which were determined at different times by different researchers who used different methods, vary in a wide range. A description of an original method of measurement of the heat flux relaxation time and the methods used by Grassmann [23], Herwig [24], Kaminski [25], and Mitra [26] can be found in [27]. Interestingly enough, the values of τ for the same materials determined by the listed researchers differ by almost two orders of magnitude, whereas the values of the thermal diffusivity determined by these researchers are sufficiently close. The values of τ for nitrogen, which are presented in [19–21], vary in the range from 0.1 ns to 10 ns. In accordance with the experimental results given in [28,29], values of τ for metals are of about tens of nanoseconds, whereas according to [30–32] values of τ for metals are of about 0.01 ns. The heat flux relaxation time for gold is determined in [33] by two methods. The first method, which is based on the consideration of phonon-phonon scattering, gives $\tau = 12$ ps. The second method, which is based on the consideration of electron-phonon scattering, gives $\tau = 1.52$ ps. According to data presented in [34], values of the heat flux relaxation time for homogeneous substances in different aggregative states vary in the range from 10 fs to 10 ns. However, in accordance with [35], the heat flux relaxation time for diamonds is of about 1 ms (the measurement was fulfilled at the temperature of liquid nitrogen, namely 77 K). In the case of materials with

non-homogeneous structure (such as soda, sand and meat), values of τ are of about seconds and tens of seconds. For example, values of τ determined in [27] are 0.66 s for soda and 2.26 s for sand. In [26], it is determined that the value of τ for meat is of about 15 s. Experiments with agar-gelled water [36] gave $\tau = 7.96$ s. Keeping all the aforesaid facts in view, we conclude that though the problem of experimental determination of the heat flux relaxation time arose a long time ago, this problem has not been finally solved up to now, and in a number of cases values of τ presented in literature are not reliable. That is why, a problem of development of theoretical foundations for new methods of experimental determination of the heat flux relaxation time has so far been important.

The model of elastic heat-conducting medium based on the Cattaneo–Vernotte heat conduction law was suggested by Lord and Shulman [37]. Subsequently, Green and Lindsay [38] suggested a theory with two relaxation parameters. In addition, Hetnarski and Ignaczak [39] suggested a theory of thermoelasticity with the specific heat nonlinearly dependent on temperature that takes palace in the case of low temperatures. We also refer to the Green–Nagdi theory of thermoelasticity [40] based on the generalized Fourier law, the right-hand side of which contains an additional term with the gradient of temperature shift proportional to mean free path. Some other non-classical models of thermal conductivity, thermoelasticity and thermoviscoelasticity are presented in the modern literature; see [41–47]. An overview of hyperbolic theories of thermoelasticity can be found in [3]. An overview of some other non-classical theories of thermoelasticity can be found in [2].

In what follows, the Maxwell-Cattaneo heat conduction theory, the Lord–Shulman model of thermoelasticity and the model of thermoviscoelasticity suggested in [44] are considered. The properties of these models, which become apparent at the nanoscale level, are studied. An asymptotic analysis of the dispersion relations is carried out and the simple formulas approximated the dispersion curves in the whole range of frequencies are suggested. In contrast to [48,49], where the dispersion relations for the solutions decaying in space are considered, we study the dispersion relations for the solutions decaying in time. Based on the results of analysis of the hyperbolic heat conduction problem, we work out the theoretical foundations of the method for measuring the heat flux relaxation time. Comparing solutions of the heat conduction problem and the appropriate coupled problem of thermoelasticity, we show that the elastic and thermal strains will not affect the accuracy of determination of the heat flux relaxation time by the suggested method.

2 The hyperbolic heat conduction equation

2.1 Dispersion curves for the Maxwell–Cattaneo heat conduction equation

We assume that there is no heat supply from the environment and the temperature varies only along the direction of the x-coordinate. Then Eq. (4) takes the form

$$\frac{\partial^2 \tilde{T}}{\partial x^2} - \frac{1}{\tau c_r^2} \frac{\partial \tilde{T}}{\partial t} - \frac{1}{c_r^2} \frac{\partial^2 \tilde{T}}{\partial t^2} = 0, \qquad c_r^2 = \frac{\lambda}{\rho c_v \tau}. \tag{5}$$

Here, c_r is the propagation velocity of thermal waves. It is easy to see that the coefficient of the term containing the first time derivative of the temperature does not depend on the parameter τ. Indeed, $\tau c_r^2 = \lambda/(\rho c_v)$.

We start with the analysis of dispersion relations. Let us look for a solution of Eq. (5) in the form

$$\tilde{T}(x, t) = \tilde{T}_0 \, e^{-i\delta x} \, e^{(-\alpha + i\omega)t}, \tag{6}$$

where δ is the wavenumber, ω is the frequency, α is the attenuation factor. Substituting Eq. (6) into Eq. (5) and separating the real and imaginary parts of the obtained equation, we get the following dispersion relations:

$$\begin{aligned} \omega \neq 0: \quad & \alpha = \frac{1}{2\tau}, \quad \omega = \sqrt{c_r^2 \delta^2 - \frac{1}{4\tau^2}}, \quad \delta \geq \delta_0 = \frac{1}{2c_r\tau}; \\ \omega = 0: \quad & \alpha^{(1,2)} = \frac{1}{2\tau} \mp \sqrt{\frac{1}{4\tau^2} - c_r^2 \delta^2}, \quad \delta \leq \delta_0 = \frac{1}{2c_r\tau}. \end{aligned} \tag{7}$$

Figure 1 shows the dispersion curves corresponding to Eq. (7). The frequency–wavenumber spectrum is shown in the diagram on the left-hand side of Fig. 1, where the dashed line corresponds to the asymptote $\omega = c_r \delta$. It is easy to see that the dispersion curve possesses the cut-off wavenumber δ_0, i.e. oscillations are absent ($\omega = 0$) when $0 \leq \delta \leq \delta_0$. The wavenumber dependence of the attenuation factor is shown in the
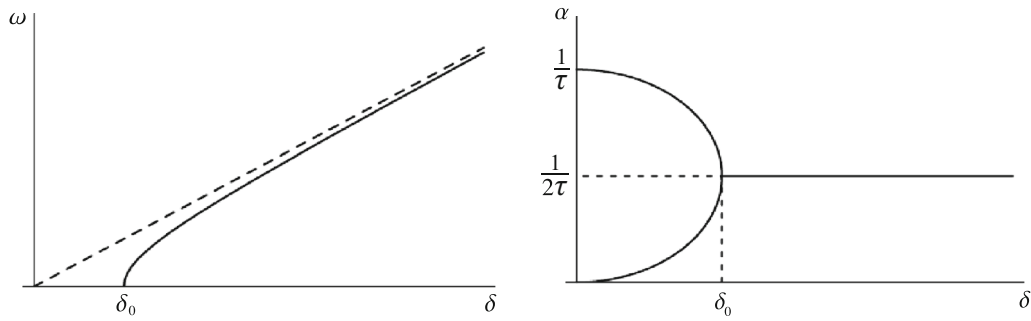
Fig. 1 The wavenumber dependence of the frequency and the attenuation factor for the Maxwell–Cattaneo heat conduction equation
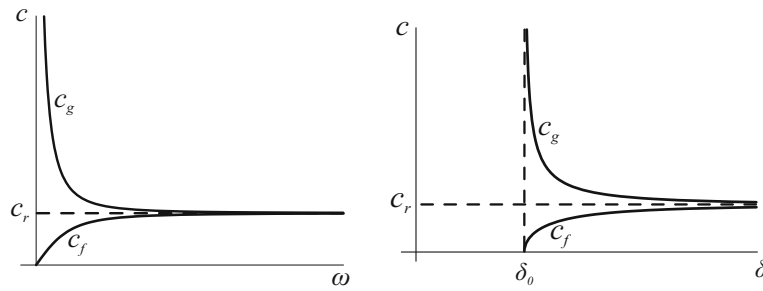
Fig. 2 The frequency and wavenumber dependences of the phase velocity and the group velocity

diagram on the right-hand side of Fig. 1. It is easy to see that two values of α correspond to each value of δ in the interval $0 \leq \delta \leq \delta_0$. One of the dispersion curves starts at point $\delta = 0$, $\alpha = 0$ and increases with increasing δ. The second dispersion curve starts at point $\delta = 0$, $\alpha = 1/\tau$ and decreases with increasing δ. The curves meet at the point $\delta = \delta_0$, $\alpha = 1/(2\tau)$. In the interval $\delta \geq \delta_0$ (where $\omega \neq 0$, see Fig. 1), the attenuation factor α does not depend on δ. This part of the dispersion curve is the straight line $\alpha = 1/(2\tau)$ in the diagram on the right-hand side of Fig. 1. If the inertial term in Eq. (5) was absent, a dispersion relation between α and δ would be $\alpha = \tau c_r^2 \delta^2$. This dependence is a good approximation for the dispersion curve starting at zero (see the diagram on the left-hand side of Fig. 1). Thus, Eq. (5) demonstrates the properties of the classical heat conduction equation for wavenumbers smaller than the cut-off wavenumber δ_0, whereas for wavenumbers greater than the cut-off wavenumber δ_0 it demonstrates the properties of the wave equation.

In accordance with Eq. (7), the expressions for the phase velocity C_f and the group velocity C_g have the form

$$C_f = \frac{\omega}{\delta}, \qquad C_f(\omega) = \frac{c_r}{\sqrt{1 + \dfrac{1}{4\omega^2\tau^2}}}, \qquad C_f(\delta) = c_r\sqrt{1 - \frac{1}{4\tau^2 c_r^2 \delta^2}},$$

$$C_g = \frac{d\omega}{d\delta}, \qquad C_g(\omega) = c_r\sqrt{1 + \frac{1}{4\omega^2\tau^2}}, \qquad C_g(\delta) = \frac{c_r}{\sqrt{1 - \dfrac{1}{4\tau^2 c_r^2 \delta^2}}}. \tag{8}$$

The frequency and wavenumber dependences of C_f and C_g are shown in Fig. 2. It is easy to see that the phase and group velocities asymptotically approach to c_r with increasing frequency (wavenumber). When $\omega = 0$, the phase velocity becomes zero and the group velocity tends to infinity. The same behavior of C_f and C_g can be observed when $\delta = \delta_0$.

A wave solution of Eq. (5) can be represented as a sum of forward and reverse traveling waves

$$\tilde{T}(x, t) = \left[A_1 \sin\left(\frac{1}{c_r}\sqrt{\omega^2 + \frac{1}{4\tau^2}}\, x - \omega t \right) + + A_2 \sin\left(\frac{1}{c_r}\sqrt{\omega^2 + \frac{1}{4\tau^2}}\, x + \omega t \right) \right] e^{-t/(2\tau)}, \tag{9}$$

or as a sum of two standing waves

$$\tilde{T}(x,t) = \left[B_1 \sin\left(\frac{1}{c_r} \sqrt{\omega^2 + \frac{1}{4\tau^2}} \, x \right) \cos(\omega t) \right.$$
$$\left. + B_2 \cos\left(\frac{1}{c_r} \sqrt{\omega^2 + \frac{1}{4\tau^2}} \, x \right) \sin(\omega t) \right] e^{-t/(2\tau)}. \tag{10}$$

A non-wave solution of Eq. (5) has the form

$$\tilde{T}(x,t) = C_1 \sin(\delta x) \left(e^{-\alpha^{(1)}t} + e^{-\alpha^{(2)}t} \right)$$
$$+ C_2 \cos(\delta x) \left(e^{-\alpha^{(1)}t} - e^{-\alpha^{(2)}t} \right). \tag{11}$$

Here, A_i, B_i, C_i are arbitrary constants. We note that the solution (10), (11) is suitable for analysis of thermal processes in finite-sized bodies when perturbations are caused, e.g., by initial conditions.

2.2 A hyperbolic heat conduction process in a thin rigid layer

We consider a heat-conducting rigid layer of thickness l. We assume that the temperature $\tilde{T}(x,t)$ of the layer is a function of time and x-coordinate directed along the thickness of the layer, i.e., $0 \leq x \leq l$. There is no external body heat supply. The boundaries of the layer are in the thermal contact with the environment. The exterior temperature is assumed to be constant and equal to T_*. The space distribution of temperature $T_0(x)$ and the space distribution of the rate of temperature change $\dot{T}_0(x)$ are known at the initial moment of time. The boundary conditions for the variable $\tilde{T} = T - T_*$ are homogeneous, namely

$$\tilde{T}\big|_{x=0} = 0, \qquad \tilde{T}\big|_{x=l} = 0. \tag{12}$$

The initial conditions for the variable $\tilde{T}$ are

$$\tilde{T}\big|_{t=0} = \tilde{T}_0(x), \qquad \dot{\tilde{T}}\big|_{t=0} = \dot{\tilde{T}}_0(x). \tag{13}$$

A solution of the problem (5), (12), (13) can be represented as a series of natural modes

$$\tilde{T}(x,t) = \sum_{k=1}^{\infty} \tilde{T}_k \, \sin \frac{\pi k x}{l} \, e^{(-\alpha_k + i\,\omega_k)\,t}, \tag{14}$$

where ω_k are the eigenfrequencies and α_k are the attenuation factors. It is easy to see that Eq. (14) identically satisfies the boundary conditions (12). Substituting Eq. (14) into Eq. (5), after simple transformations we obtain

$$k < k_* : \quad \omega_k = 0, \quad \alpha_k^{(1,2)} = \frac{1}{2\tau} \mp \sqrt{\frac{1}{4\tau^2} - \left(\frac{\pi k c_r}{l} \right)^2};$$
$$k \geq k_* : \quad \alpha_k = \frac{1}{2\tau}, \quad \omega_k = \sqrt{\left(\frac{\pi k c_r}{l} \right)^2 - \frac{1}{4\tau^2}}, \quad k_* = 1 + \left[\frac{l}{2\pi c_r \tau} \right], \tag{15}$$

where square brackets in the expression for k_* denote the integer part of the expression.

Now, in view of Eq. (15), we rewrite the series (14) as

$$\tilde{T}(x,t) = \sum_{k=1}^{k_*-1} \left(\tilde{T}_k^{(1)} e^{-\alpha_k^{(1)}t} + \tilde{T}_k^{(2)} e^{-\alpha_k^{(2)}t} \right) \sin \frac{\pi k x}{l}$$
$$+ e^{-t/(2\tau)} \sum_{k=k_*}^{\infty} \left(\tilde{T}_k^{(1)} \cos(\omega_k t) + \tilde{T}_k^{(2)} \sin(\omega_k t) \right) \sin \frac{\pi k x}{l}. \tag{16}$$

Let us find the coefficients of the series (16) taking into account the initial conditions (13). At first, we suppose that $\dot{\tilde{T}}_0(x) \ll \tilde{T}_0(x)/\tau$. In this case, the coefficients are calculated by the formulas

$$
\begin{aligned}
& \tilde{T}_k^{(1)} \approx \frac{2}{l} \int_0^l \tilde{T}_0(x) \sin \frac{\pi kx}{l} \, dx; \\
& k < k_*: \ \tilde{T}_k^{(2)} \approx 0, \qquad k \geq k_*: \ \tilde{T}_k^{(2)} \approx \frac{1}{2\tau\omega_k} \tilde{T}_k^{(1)}.
\end{aligned} \tag{17}
$$

Next, we suppose that $\dot{\tilde{T}}_0(x) \sim \tilde{T}_0(x)/\tau$. In this case, the coefficients are calculated by the formulas

$$
\begin{aligned}
& k < k_*: \ \tilde{T}_k^{(2)} \approx \frac{2}{l\alpha_k^{(2)}} \int_0^l \dot{\tilde{T}}_0(x) \sin \frac{\pi kx}{l} \, dx, \\
& \tilde{T}_k^{(1)} \approx -\tilde{T}_k^{(2)} + \frac{2}{l} \int_0^l \tilde{T}_0(x) \sin \frac{\pi kx}{l} \, dx; \\
& k \geq k_*: \ \tilde{T}_k^{(1)} = \frac{2}{l} \int_0^l \tilde{T}_0(x) \sin \frac{\pi kx}{l} \, dx, \\
& \tilde{T}_k^{(2)} = \frac{1}{\omega_k} \left[\frac{1}{2\tau} \tilde{T}_k^{(1)} + \frac{2}{l} \int_0^l \dot{\tilde{T}}_0(x) \sin \frac{\pi kx}{l} \, dx \right].
\end{aligned} \tag{18}
$$

Now we discuss the influence of the scale factor l on the solution of free oscillation problem. A numerical analysis was carried out for copper layers of various thicknesses. According to some theoretical and experimental studies, the values of the heat flux relaxation time for metals are in the range from 0.1 ns to 100 ns. That is why, to study the influence of the scale factor l on the solution of the heat conduction problem we considered four values of τ, namely 0.1, 1, 10 and 100 ns. As seen from Eq. (15), there exists the number k_*, such as for $k \geq k_*$ the solution has the oscillatory character, and both the number k_* and the value of ω_{k_*} depend on the layer thickness l. Results of the numerical analysis are in Tables 1, 2, 3, and 4, which contain the following data. The layer thickness and the number of the first oscillating mode k_* are in the first and second columns. The third column contains the inverse quantity of wavenumber, which is calculated as $l/(\pi k_*)$ for

Table 1 The dependence of the solution on the scale factor l in the case of copper when $\tau = 0.1$ ns

l (μm)	k_*	$l/(\pi k_*)$ (μm)	ω_{k_*} (rad/ns)	$\alpha_{k_*}/\omega_{k_*}$	$\alpha_{k_*}/\alpha_1^{(1)}$
10^6	1466586	0.217	2890	1732.9	4.30×10^{12}
1000	1467	0.217	11.9	42.07	4.30×10^6
100	147	0.217	34.1	14.65	4307.0
10	15	0.212	1.07	4.66	429.67
5	8	0.199	2.18	2.29	107.04
4	6	0.212	1.07	4.66	68.32
3	6	0.185	3.03	1.65	52.19
1	2	0.159	4.64	1.079	3.72
0.1	1	0.0318	0.337	0.1483	—
0.01	1	0.00318	0.0341	0.0147	—

Table 2 The dependence of the solution on the scale factor l in the case of copper when $\tau = 1$ ns

l (μm)	k_*	$l/(\pi k_*)$ (μm)	ω_{k_*} (rad/ns)	$\alpha_{k_*}/\omega_{k_*}$	$\alpha_{k_*}/\alpha_1^{(1)}$
10^6	463776	0.686	96400	518.43	4.30×10^{11}
1000	464	0.686	156	32.11	4.30×10^{05}
100	47	0.677	822	6.08	4301.25
10	5	0.637	20.1	2.48	42.51
5	3	0.531	41.0	1.22	10.23
4	2	0.637	20.1	2.48	6.34
3.5	2	0.557	36.0	1.39	4.71
1	1	0.318	95.5	0.523	—
0.1	1	0.0318	0.18	0.0464	—
0.01	1	0.00318	0.0108	0.0046	—

Table 3 The dependence of the solution on the scale factor l in the case of copper when $\tau = 10\,\text{ns}$

l (µm)	k_*	$l/(\pi k_*)$ (µm)	ω_{k_*} (rad/ns)	$\alpha_{k_*}/\omega_{k_*}$	$\alpha_{k_*}/\alpha_1^{(1)}$
10^6	146659	2.17	12000	415.66	4.30×10^{10}
1000	147	2.17	3410	14.65	4.30×10^4
100	15	2.12	107	4.66	429.67
10	2	1.59	464	1.08	3.72
5	1	1.59	464	1.08	—
4	1	1.27	690	0.72	—
3.5	1	1.11	836	0.60	—
1	1	0.318	33.7	0.148	—
0.1	1	0.0318	3.41	0.0147	—
0.01	1	0.00318	0.341	0.0015	—

Table 4 The dependence of the solution on the scale factor l in the case of copper when $\tau = 100\,\text{ns}$

l (µm)	k_*	$l/(\pi k_*)$ (µm)	ω_{k_*} (rad/ns)	$\alpha_{k_*}/\omega_{k_*}$	$\alpha_{k_*}/\alpha_1^{(1)}$
10^6	46378	6.86	229000	218.37	4.30×10^9
1000	47	6.77	82200	6.08	4.30×10^3
100	5	6.37	2010	2.48	42.51
10	1	3.18	9550	0.52	—
5	1	1.59	210	0.24	—
4	1	1.27	265	0.19	—
3.5	1	1.11	304	0.16	—
1	1	0.318	10.8	0.046	—
0.1	1	0.0318	1.08	0.0046	—
0.01	1	0.00318	0.108	0.0005	—

the considered boundary conditions. The value of the eigenfrequency ω_{k_*} and the ratio of the attenuation factor $\alpha_{k_*} = 1/(2\tau)$ to the eigenfrequency ω_{k_*} are in the fourth and fifth columns. The ratio of the attenuation factor α_{k_*} to the attenuation factor $\alpha_1^{(1)}$ of the first normal mode is in the sixth column. These results show that at the macro level the oscillation processes are not of interest since they appear at very large values of k_*. When the heat flux relaxation time increases, the oscillatory solutions appear at greater values of l for the given value of k_* and at smaller values of k_* for the given value of l. In the case of $\tau = 0.1\,\text{ns}$ (see Table 1), the oscillatory solutions appear at small values of k_* if the layer thickness l is smaller than $5\,\mu\text{m}$. In the case of $\tau = 100\,\text{ns}$ (see Table 4), the oscillatory solutions appear at small values of k_* if the layer thickness l does not exceed $100\,\mu\text{m}$. However, the oscillation process can evolve over some time only when the ratio of the attenuation factor α_{k_*} to the eigenfrequency ω_{k_*} is less than unity. Thus, the oscillatory character of the heat conduction equation can become apparent only when $l \sim 0.1\,\mu\text{m}$ for $\tau = 0.1\,\text{ns}$ (see Table 1) and when $l \sim 10\,\mu\text{m}$ for $\tau = 100\,\text{ns}$ (see Table 4).

The diagrams in Figs. 3 and 4 illustrate the solution of the Maxwell–Cattaneo hyperbolic heat conduction problem (5), (12), (13). The calculations were carried out for the copper layer in the case of the initial distribution of temperature $\tilde{T}_0(x) = \tilde{T}_0 \sin \dfrac{\pi k x}{l}$, when the initial value of $\dot{\tilde{T}}$ is equal to zero. The diagrams in Fig. 3a,c and Fig. 4a, c correspond to $k = 1$. The diagrams in Fig. 3b, d and Fig. 4b, d correspond to $k = 2$. Two values of the heat flux relaxation time, namely $\tau = 0.1\,\text{ns}$ (see Fig. 3) and $\tau = 1\,\text{ns}$ (see Fig. 4), and four values of the layer thickness l were considered. The diagrams in Fig. 3a, b and Fig. 4c,d correspond to $l = 1\,\mu\text{m}$, the diagrams in Fig. 3c, d correspond to $l = 0.1\,\mu\text{m}$, and the diagrams in Fig. 4a, b correspond to $l = 3.5\,\mu\text{m}$. The diagrams in Fig. 3 show that in the case of copper with $\tau = 0.1\,\text{ns}$ the conversion from the monotone decreasing solution to the solution that decreases with oscillations occurs when the layer thickness l is in the range from $0.1\,\mu\text{m}$ to $1\,\mu\text{m}$. In accordance with data in Table 1, if $l = 1\,\mu\text{m}$, then the monotone decreasing solution takes place only for the first mode ($k = 1$, see Fig. 3a), whereas in the case of the second mode ($k = 2$, see Fig. 3b) the solution decreases with oscillations. However, in the case of the oscillatory solution, the oscillations cannot be observed because of the ratio α/ω is too large (greater than unity). When $l = 0.1\,\mu\text{m}$, the strongly pronounced oscillations can be observed for both the first mode (Fig. 3c) and the second mode (Fig. 3d). If $\tau = 1\,\text{ns}$, then the boundary between the monotone decreasing solution (Fig. 4a) and the solution decreasing with oscillations
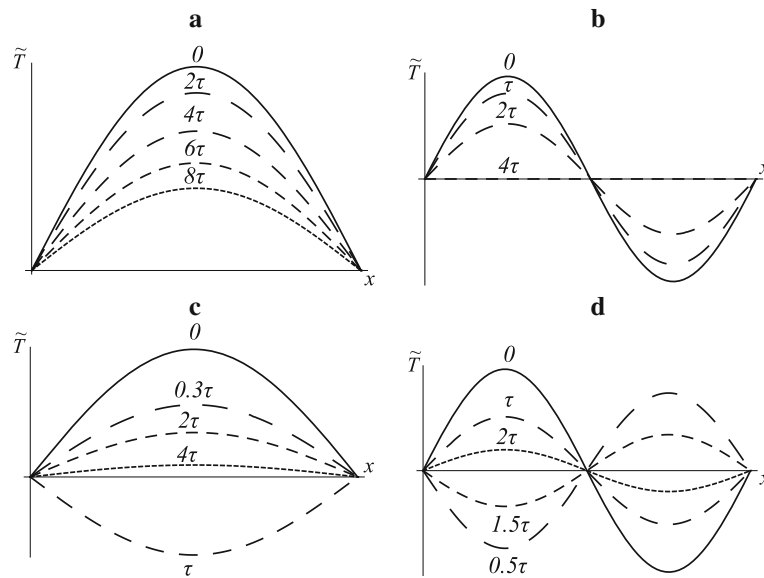
Fig. 3 The temperature distribution in the copper layer when $\tau = 0.1\,\text{ns}$
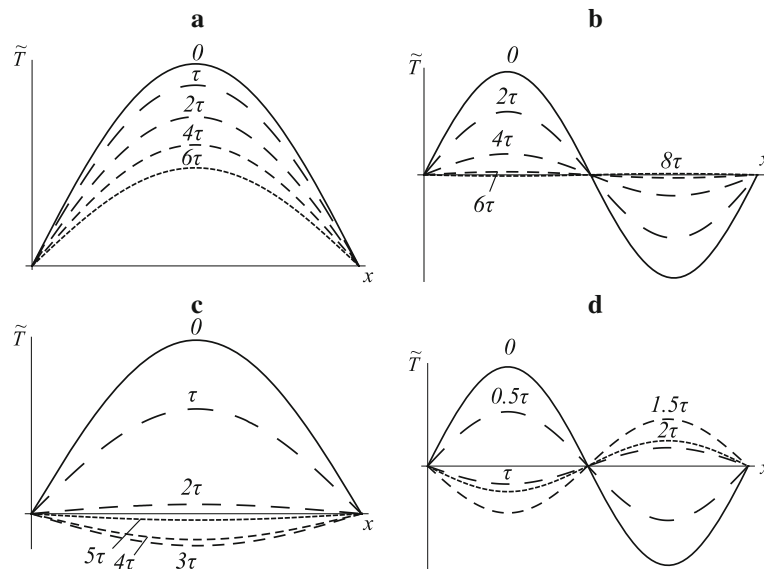
Fig. 4 The temperature distribution in the copper layer when $\tau = 1\,\text{ns}$

(Fig. 4b–d) is in the range from $l = 1\,\mu\text{m}$ to $l = 3.5\,\mu\text{m}$. This fact is confirmed by the data presented in Table 2.

2.3 An idea on experimental determination of the heat flux relaxation time

The effect described above, namely the appearance of oscillations in the decreasing solution when the layer thickness becomes smaller, allows us to suggest an experimental method of determination of the heat flux relaxation time. The idea consists in the following strategy. We should take a plate of thickness l and specify the initial distribution of temperature in the direction along the plate thickness as $\tilde{T}_0(x) = \tilde{T}_0 \sin(\delta_k x)$, where $\delta_k = \pi k / l$ and $0 \leq x \leq l$. Next, we should find out what is the character of temperature changing. If the temperature monotone decreases, then $\delta_k < \delta_0$. If the temperature decreases with oscillations then $\delta_k > \delta_0$. Next, we should reiterate this experiment for plates of different thickness l in order to determine the value of

the cut-off wavenumber δ_0 as accurately as possible. According to Eqs. (5), (7), we have

$$\delta_0 = \frac{1}{2c_r\tau}, \qquad c_r^2 = \frac{\lambda}{\rho c_v \tau}. \tag{19}$$

Eliminating c_r from Eq. (19), we get

$$\tau = \frac{\rho c_v}{4\lambda\delta_0^2}. \tag{20}$$

Thus, if the value of δ_0 is determined experimentally, then the heat flux relaxation time τ can be calculated by Eq. (20).

3 Hyperbolic thermoelasticity

3.1 A statement of the coupled problem of hyperbolic thermoelasticity

Now, we write down the system of equations of the Lord–Shulman theory of thermoelasticity [37]. The equation of motion has the form

$$\nabla \cdot \boldsymbol{\tau} + \rho \mathbf{f} = \rho \ddot{\mathbf{u}}, \tag{21}$$

where $\boldsymbol{\tau}$ is the stress tensor, $\mathbf{f}$ is the mass density of external actions, and $\mathbf{u}$ is the displacement vector. The constitutive equation for the stress tensor is

$$\boldsymbol{\tau} = \left(K - \frac{2}{3}G \right) \varepsilon \mathbf{E} + 2G\boldsymbol{\varepsilon} - \alpha_* K \tilde{T} \mathbf{E}, \tag{22}$$

where $\mathbf{E}$ is the unit tensor, $\boldsymbol{\varepsilon}$ is the strain tensor, ε is the trace of the strain tensor, K is the isothermal bulk modulus, G is the shear modulus, and α_* is the volume thermal expansion coefficient. Equation (22) is known as the Duhamel–Neumann law. In the linear theory, the expressions for the stress tensor and the trace of the strain tensor have the form

$$\boldsymbol{\varepsilon} = \frac{1}{2}(\nabla\mathbf{u} + \nabla\mathbf{u}^T), \qquad \varepsilon \equiv \mathrm{tr}\,\boldsymbol{\varepsilon} = \nabla \cdot \mathbf{u}. \tag{23}$$

Substituting Eq. (22) into Eq. (21), we obtain the equation of motion in the form

$$G\Delta\mathbf{u} + \left(K + \frac{1}{3}G \right) \nabla\nabla \cdot \mathbf{u} - \alpha_* K \nabla\tilde{T} = \rho\ddot{\mathbf{u}}. \tag{24}$$

In the coupled problem of thermoelasticity, the classical heat conduction equation has the form

$$\lambda\Delta\tilde{T} - \rho c_v \dot{\tilde{T}} - \alpha_* K T_* \dot{\varepsilon} + \rho q = 0, \tag{25}$$

The heat conduction equation taking into account the finiteness of the heat flux relaxation time τ has the form

$$\lambda\Delta\tilde{T} - \rho c_v \left(\dot{\tilde{T}} + \tau\ddot{\tilde{T}} \right) - \alpha_* K T_* \left(\dot{\varepsilon} + \tau\ddot{\varepsilon} \right) + \rho \left(q + \tau\dot{q} \right) = 0. \tag{26}$$

It is known that in the linear theory the differential equation describing the transverse waves does not depend on temperature, see [50]. That is why, below we consider only the longitudinal waves associated with the volume strains. Taking the divergence of Eq. (24) and taking into account the second equation in Eq. (23), we obtain

$$\left(K + \frac{4}{3}G \right) \Delta\varepsilon - \alpha_* K \Delta\tilde{T} = \rho\ddot{\varepsilon} \tag{27}$$

Thus, the system of equations of the coupled problem of thermoelasticity, taking into account the finiteness of the heat flux relaxation time τ, consists of the equation of motion (27) and the heat conduction Eq. (26). It is easy to see that when the parameter τ vanishes this system of equations turns into the system of equations of the classical theory of thermoelasticity (25), (27).

3.2 An analysis of dispersion relations in the coupled problem of thermoelasticity

In order to analyze the dispersion relations, we consider a one-dimensional problem of the thermoelastic wave propagation in the direction of x-coordinate. The external actions and the body heat supply from external sources are assumed to be equal to zero. In this case, Eqs. (26), (27) take the form

$$\frac{\partial^2 \tilde{T}}{\partial x^2} - \frac{\rho c_v}{\lambda}\left(\frac{\partial \tilde{T}}{\partial t} + \tau \frac{\partial^2 \tilde{T}}{\partial t^2}\right) = \frac{\alpha_* K T_*}{\lambda}\left(\frac{\partial \varepsilon}{\partial t} + \tau \frac{\partial^2 \varepsilon}{\partial t^2}\right), \tag{28}$$

$$\left(K + \frac{4}{3}G\right)\frac{\partial^2 \varepsilon}{\partial x^2} - \alpha_* K \frac{\partial^2 \tilde{T}}{\partial x^2} = \rho \frac{\partial^2 \varepsilon}{\partial t^2}. \tag{29}$$

After simple transformations, Eqs. (28), (29) can be reduced to one differential equation in the variable ε (or the exactly same equation in variable $\tilde{T}$), namely

$$\frac{\partial^4 \varepsilon}{\partial x^4} - (A_1 + A_2)\frac{\partial^4 \varepsilon}{\partial t^2 \partial x^2} - A_3 \frac{\partial^3 \varepsilon}{\partial t \partial x^2} +$$
$$+ A_1 A_3 (1 - A_4)\frac{\partial^3 \varepsilon}{\partial t^3} + A_1 A_2 (1 - A_4)\frac{\partial^4 \varepsilon}{\partial t^4} = 0, \tag{30}$$

where the following notations are used:

$$A_1 = \frac{\rho}{K + \frac{4}{3}G}, \qquad A_3 = \frac{1}{\lambda}\left(\rho c_v + \frac{\alpha_*^2 K T_*}{1 + \frac{4}{3}GK^{-1}}\right),$$
$$A_2 = \tau A_3, \qquad A_4 = \frac{1}{1 + \rho c_v (1 + \frac{4}{3}GK^{-1})/(\alpha_*^2 K T_*)}. \tag{31}$$

All the quantities A_i in Eq. (31) are strictly positive. The parameter A_4 varies in the range from 0 to 1, and for solids and liquids $A_4 \ll 1$, whereas for gases $A_4 > 1/2$. The parameter A_1 characterizes the acoustic wave propagation velocity: $c_a = 1/\sqrt{A_1(1 - A_4)}$. The parameter A_2 characterizes the thermal wave propagation velocity: $c_r = 1/\sqrt{A_2}$.

The classical analogue of Eq. (30) follows from this equation if the heat flux relaxation time is assumed to be equal to zero, i.e., when $A_2 = 0$:

$$\frac{\partial^4 \varepsilon}{\partial x^4} - A_1 \frac{\partial^4 \varepsilon}{\partial t^2 \partial x^2} - A_3 \frac{\partial^3 \varepsilon}{\partial t \partial x^2} + A_1 A_3 (1 - A_4)\frac{\partial^3 \varepsilon}{\partial t^3} = 0. \tag{32}$$

The difference between Eqs. (30) and (32) consists in the fact that Eq. (30) contains the fourth-order time derivative.

In order to obtain the dispersion relations, we can look for a solution of Eq. (30) in the form of an exponential function decreasing in space coordinate:

$$\varepsilon(x, t) = \varepsilon_0 \, e^{(-\gamma + i\delta)x} \, e^{-i\omega t}, \tag{33}$$

where γ is the attenuation factor, δ is the wavenumber, and ω is the frequency. This approach is suitable in the case when we compare the values of a physical quantity at different points of space in order to experimentally estimate the attenuation factor. A detailed analysis of the respective dispersion relations can be found in [48,49].

Now, we look for a solution of Eq. (30) in the form of an exponential function decreasing in time:

$$\varepsilon(x, t) = \varepsilon_0 \, e^{-i\delta x} \, e^{(-\alpha + i\omega)t}, \tag{34}$$

where δ is the wavenumber, ω is the frequency, and α is the attenuation factor. This approach is suitable in the case when we compare the values of a physical quantity at different moments of time in order to experimentally estimate the attenuation factor.

Substituting Eq. (34) into Eq. (30) and separating the obtained equation into real and imaginary parts, we come to the following dispersion relations between δ, ω and α:
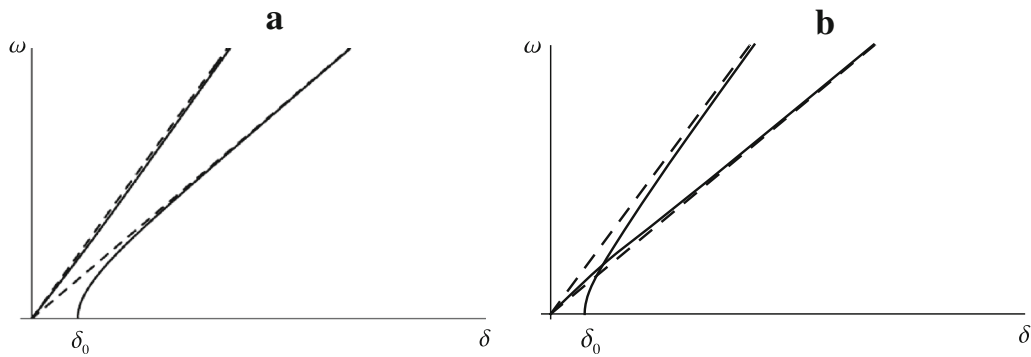
Fig. 5 The wavenumber dependence of the frequency: **a** $c_a > c_r$; **b** $c_a < c_r$

$$\delta^4 + \big((A_1 + A_2)(\alpha^2 - \omega^2) - A_3\alpha\big)\delta^2 +$$
$$+A_1(1 - A_4)\big(A_2(\alpha^4 - 6\alpha^2\omega^2 + \omega^4) + A_3\alpha(3\omega^2 - \alpha^2)\big) = 0,$$
$$\omega\Big((2(A_1 + A_2)\alpha - A_3)\,\delta^2 + A_1(1-A_4)\big(4A_2\alpha(\alpha^2 - \omega^2) + A_3(\omega^2 - 3\alpha^2)\big)\Big) = 0. \tag{35}$$

The dispersion curves corresponding to Eq. (35) are shown in Figs. 5, 6, 7, 8. The dependence of the frequency ω on the wavenumber δ is shown in Fig. 5. The almost straight line starting from point $\delta = 0$ represents the acoustic spectrum. This spectrum exists in both the hyperbolic thermoelasticity and the classical thermoelasticity. The curve starting from point $\delta = \delta_0$ represents the thermal spectrum. This spectrum exists in the hyperbolic thermoelasticity due to the theory takes into account the inertia terms in the heat conduction equation. In the case when the acoustic wave velocity c_a is smaller than the thermal wave velocity c_r, the dispersion curves have a common point (see Fig. 5 b). Both the dispersion curves have asymptotes, which are shown in Fig. 5 by dashed lines. Equations of the asymptotes are

$$\delta_a = \sqrt{-\frac{c}{c_1}}\,\omega_a, \qquad \delta_h = \sqrt{\frac{c}{c_2}}\,\omega_h. \tag{36}$$

Here, the acoustic and thermal spectra are denoted by the indexes "a" and "h", respectively. In the case of $c_a > c_r$, the constants c_1 and c_2 are calculated as

$$c_{1,2} = \mp \frac{A_1 A_3^3 A_4(A_2 - A_1 + 2A_1A_4)}{4A_2((A_1 - A_2)^2 + 4A_1A_2A_4)^{5/2}}\Big[A_1 +$$
$$+A_2 \pm \sqrt{(A_1 - A_2)^2 + 4A_1A_2A_4}\Big]. \tag{37}$$

In the case of $c_a < c_r$, the constants c_1 and c_2 are calculated as

$$c_{1,2} = \pm \frac{A_1 A_3^3 A_4(A_2 - A_1 + 2A_1A_4)}{4A_2((A_1 - A_2)^2 + 4A_1A_2A_4)^{5/2}}$$
$$\Big[A_1 + +A_2 \mp \sqrt{(A_1 - A_2)^2 + 4A_1A_2A_4}\Big]. \tag{38}$$

The constant c is calculated by the formula

$$c = \frac{A_1 A_2(1-A_4)(c_2 - c_1)}{A_1 + A_2}. \tag{39}$$

As seen from Eqs. (37), (38), the constant c_1 is always negative and the constant c_2 is always positive. Hence, the constant c is positive. Thus, the radical expressions in Eq. (36) are always positive. The cut-off wavenumber δ_0 is calculated by the formula

$$\delta_0 = \alpha_3 \sqrt{\frac{A_1(3A_3 - 4A_2\alpha_3)(1-A_4)}{2\,\alpha_3(A_1 + A_2) - A_3}}. \tag{40}$$
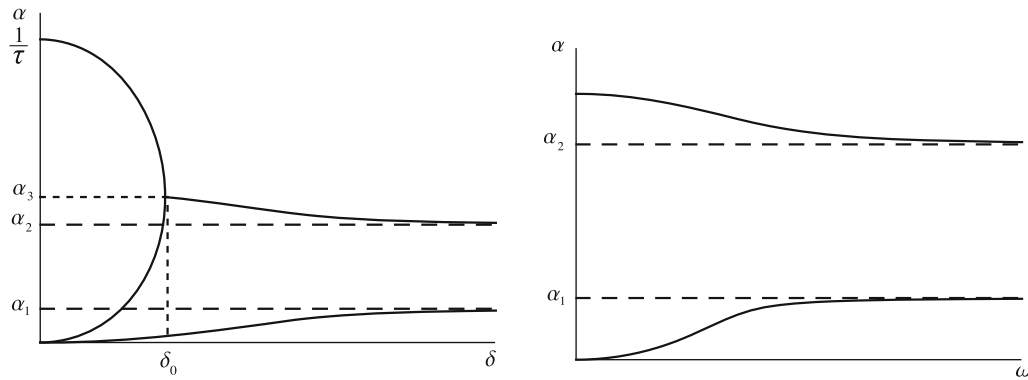
Fig. 6 The wavenumber and frequency dependences of the attenuation factor

Here, the constants α_1 and α_2 are, respectively, the smaller root and the larger root of the quadratic equation

$$4A_2\alpha^2 - 2A_3\alpha + \frac{A_1 A_3^2 A_4}{(A_1 - A_2)^2 + 4A_1 A_2 A_4} = 0. \tag{41}$$

The constant α_3 is the unique real root of the cubic equation

$$4A_2\alpha^3 - 2\left(1 + \frac{4A_2(A_2 - A_1 + 2A_1 A_4)}{(A_1 - A_2)^2 + 4A_1 A_2 A_4}\right)A_3 \alpha^2$$
$$+ \frac{8A_2 - 4A_1 + 9A_1 A_4}{(A_1 - A_2)^2 + 4A_1 A_2 A_4} A_3^2 \alpha - \frac{2A_3^3}{(A_1 - A_2)^2 + 4A_1 A_2 A_4} = 0. \tag{42}$$

The dependence of the attenuation factor α on the wavenumber δ is shown in the diagram on the left-hand side of Fig. 6. The acoustic curve starts from point $\delta = 0$, $\alpha = 0$ and tends to the asymptote $\alpha = \alpha_1$ at $\delta \to \infty$. This curve exists in both the hyperbolic thermoelasticity and the classical thermoelasticity. The remainder curves correspond to the thermal spectrum. In the interval $0 \leq \delta \leq \delta_0$ where thermal waves are absent (i.e., $\omega = 0$, see Fig. 5), two values of α correspond to each value of δ. One of the dispersion curves starts from point $\delta = 0$, $\alpha = 0$ and increases with increasing δ. The second dispersion curve starts from point $\delta = 0$, $\alpha = 1/\tau$ and decreases with increasing δ. The curves meet at point $\delta = \delta_0$, $\alpha = \alpha_3$. In the interval $\delta \geq \delta_0$ where thermal waves exist (i.e., $\omega \neq 0$, see Fig. 5), the dependence of α on δ is represented by one curve which starts from point $\delta = \delta_0$, $\alpha = \alpha_3$ and tends to the asymptote $\alpha = \alpha_2$ at $\delta \to \infty$. In the classical theory of thermoelasticity, there is only one thermal dispersion curve. It starts from point $\alpha = 0$, $\delta = 0$ and increases ad infinitum at $\delta \to \infty$. The ratio of parameters c_a and c_r has practically no effect on the behavior of the wavenumber dependence of the attenuation factor. The dependence of the attenuation factor α on the frequency ω is shown in the diagram on the right-hand side of Fig. 6. The acoustic curve starts from point $\alpha = 0$ and tends to the asymptote $\alpha = \alpha_1$ at $\omega \to \infty$. This curve exists in both the hyperbolic thermoelasticity and the classical thermoelasticity. The thermal curve starts from point $\alpha = \alpha_3$ and tends to the asymptote $\alpha = \alpha_2$ at $\omega \to \infty$. This dispersion curve is absent in the classical theory of thermoelasticity.

The frequency dependences of the phase and group velocities are shown in Figs. 7 and 8, respectively. The phase and group velocities have the same asymptotes, which are given by the formulas

$$C_a^* = \sqrt{-\frac{c_1}{c}}, \qquad C_h^* = \sqrt{\frac{c_2}{c}}, \tag{43}$$

where c_1, c_2 are calculated by Eqs. (37), (38) and c is calculated by Eq. (39). As stated above, the constant c_1 is always negative, whereas the constants c_2 and c are always positive. Hence, the radical expressions in Eq. (43) are positive. If $c_a > c_r$, then the acoustic asymptote is higher than the thermal one. If $c_a < c_r$, then the thermal asymptote is higher than the acoustic one. The acoustic phase velocity approaches to its asymptote from below if $c_a > c_r$ (see Fig. 7, a) and from above if $c_a < c_r$ (see Fig. 7b). The behavior of the thermal phase velocity does not depend on the ratio of the parameters c_a and c_r. This curve starts from zero and approaches to its asymptote from below. Due to these facts, the acoustic and thermal curves have a common point when $c_a < c_r$ (see Fig. 7b) and have no common points when $c_a > c_r$ (see Fig. 7a). In the case of group velocities,
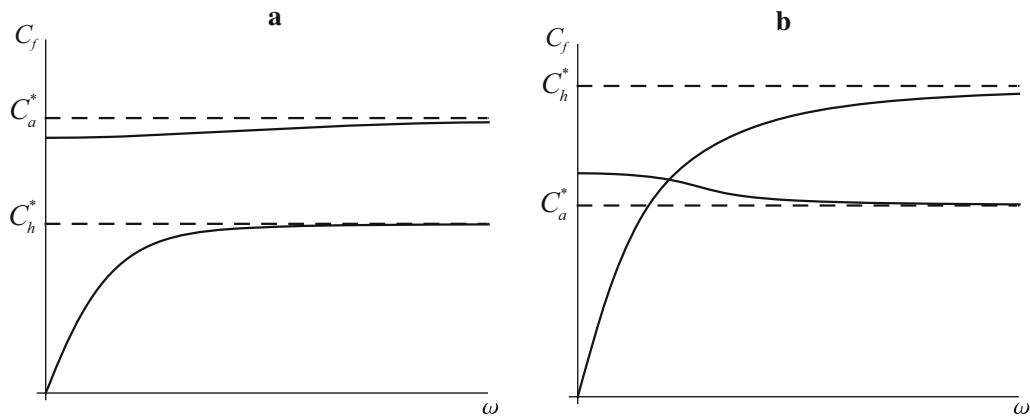
Fig. 7 The frequency dependence of the phase velocity: **a** $c_a > c_r$; **b** $c_a < c_r$
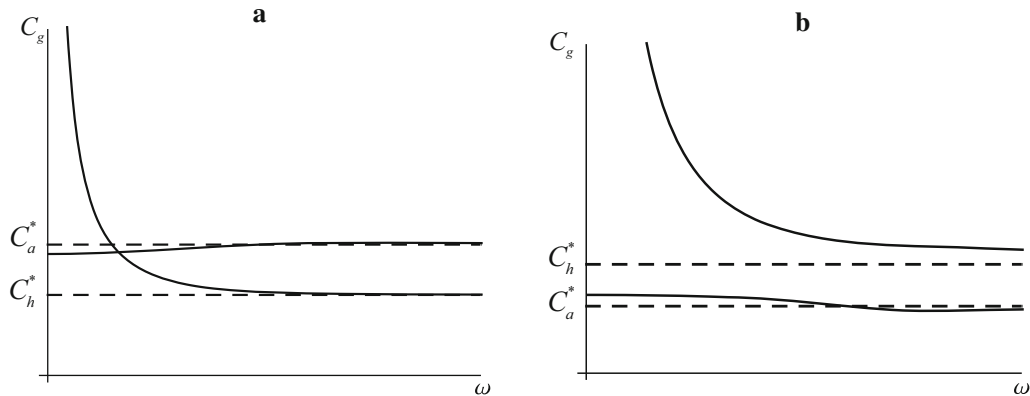
Fig. 8 The frequency dependence of the group velocity: **a** $c_a > c_r$; **b** $c_a < c_r$

on the contrary, the acoustic and thermal curves have a common point when $c_a > c_r$ (see Fig. 8a) and have no common points when $c_a < c_r$ (see Fig. 8b). This is due to the fact that the thermal curve always starts from infinity and approaches to its asymptote from above, whereas the acoustic curve is situated higher than the thermal asymptote when $c_a > c_r$ and lower than the thermal asymptote when $c_a < c_r$.

3.3 Approximate formulas for the dispersion curves

The dispersion curves shown in Figs. 5, 6, 7, 8 can be quite accurately approximated by the simple formulas, which are obtained without assuming that some parameters are small.

The approximate formulas that relate the frequency ω to the attenuation factor α (see Fig. 6) for the acoustic and thermal spectra have the form

$$\omega_a = \sqrt{\alpha \left(\frac{2A_3}{A_1 A_4} + \frac{c_1 \alpha}{\alpha_1^2 (\alpha_1 - \alpha)} \right)}, \quad \omega_h = \sqrt{\frac{c_2 (\alpha_3 - \alpha)}{(\alpha_3 - \alpha_2)(\alpha - \alpha_2)}}. \tag{44}$$

The approximate formulas that relate the wavenumber δ to the attenuation factor α (see Fig. 6) for the acoustic spectrum at all values of δ and for the thermal spectrum at $\delta \geq \delta_0$ are

$$\delta_a = \sqrt{\alpha \left(\frac{2A_3(1-A_4)}{A_4} + \frac{c\,\alpha}{\alpha_1^2 (\alpha_1 - \alpha)} \right)}, \quad \delta_h = \sqrt{\delta_0^2 + \frac{c\,(\alpha_3 - \alpha)}{(\alpha_3 - \alpha_2)(\alpha - \alpha_2)}}. \tag{45}$$

The exact formula relating the wavenumber δ to the attenuation factor α for the thermal spectrum at $\delta \leq \delta_0$ has the form

$$\delta_h = \left[\frac{\alpha}{2} \Big(A_3 - (A_1 + A_2)\,\alpha + \right.$$
$$\left. + \sqrt{\big(A_3 - (A_1 + A_2)\,\alpha\big)^2 + 4A_1\alpha(A_3 - A_2\alpha)(1 - A_4)} \Big) \right]^{1/2}. \tag{46}$$

The approximate formulas that relate the wavenumber δ to the frequency ω (see Fig. 5) for the acoustic spectrum at all values of δ and for the thermal spectrum at $\delta \geq \delta_0$ are

$$\delta_a = \omega_a \sqrt{-\frac{c}{c_1} + \frac{2A_3\alpha_1\big(c + c_1 A_1(1 - A_4)\big)}{c_1\big(2A_3\alpha_1 + A_1 A_4\,\omega_a^2\big)}}, \quad \delta_h = \sqrt{\delta_0^2 + \frac{c\,\omega_h^2}{c_2}}. \tag{47}$$

The approximate formulas expressing the frequency dependence of the phase velocity C_f and the group velocity C_g for the acoustic and thermal spectra follow from Eq. (47). They have the form

$$C_{f,a}(\omega) = \sqrt{-\frac{c_1(2A_3\alpha_1 + A_1 A_4\omega^2)}{2A_1 A_3 c_1\alpha_1(A_4 - 1) + A_1 A_4 c\omega^2}},$$

$$C_{f,h}(\omega) = \omega\sqrt{\frac{c_2}{\delta_0^2 c_2 + c\omega^2}}, \qquad C_{g,h}(\omega) = \frac{c_2}{C_{f,h}c}, \tag{48}$$

$$C_{g,a}(\omega) = -\frac{c_1(2A_3\alpha_1 + A_1 A_4\omega^2)^2}{A_1(A_1 A_4^2 c\omega^4 + 4A_3\alpha_1(A_4 c\omega^2 + A_3 c_1\alpha_1(A_4 - 1)))C_{f,a}}.$$

3.4 A hyperbolic heat conduction process in a thin elastic layer

Now, we consider a heat-conducting elastic layer of thickness l. We assume that the temperature $T(x, t)$ and the displacement $u(x, t)$ of the layer are functions of time and x-coordinate directed along the thickness of the layer ($0 \leq x \leq l$). There are no external body forces, and the body heat supply is absent. The boundaries of the layer are fixed and in the thermal contact with the environment. The exterior temperature is assumed to be constant and equal to T_*. The space distribution of temperature at the initial moment of time is given by the formula $\tilde{T}_0(x) = \tilde{T}_0 \sin \frac{\pi k x}{l}$. The initial values of the displacement, the velocity and the rate of temperature change are assumed to be equal to zero.

Figure 9 shows the comparison of the temperature profiles obtained as the solutions of two problems. One of them is the coupled problem of the Lord–Shulman thermoelasticity. The corresponding temperature profiles are shown by solid lines in Fig. 9. The second problem is the Maxwell–Cattaneo hyperbolic heat conduction problem. The corresponding temperature profiles are shown by dashed lines in Fig. 9.

The finite difference method was used to solve the coupled problem of the Lord–Shulman thermoelasticity. The explicit time integration scheme was implemented. The program was written in Delphi. The calculations were carried out for the copper layers of thickness $l = 1$ μm (Fig. 9a, b) and $l = 0.1$ μm (Fig. 9c, d). The heat flux relaxation time τ is assumed to be equal to 0.1 ns. Two different values of k were considered. The temperature profiles for $k = 1$ are shown in Fig. 9a, c. The temperature profiles for $k = 2$ are shown in Fig. 9b, d. All the diagrams correspond to the moment of time $t = 2\tau$. An analysis of the numerical results shows that the solution of the heat conduction problem practically coincides with the solution of the coupled problem of thermoelasticity. This fact is illustrated by the diagrams in Fig. 9. We note that the difference between the solutions of the heat conduction problem and the coupled problem of thermoelasticity is more noticeable in the case of the oscillatory solutions. In the case of $k = 1$, the solution of the coupled problem of thermoelasticity attenuates more quickly than the solution the heat conduction problem, whereas in the case of $k = 2$, on the contrary, the solution the heat conduction problem attenuates more quickly than the solution of the coupled problem of thermoelasticity.

The comparative analysis of the dispersion curves corresponding to the Maxwell–Cattaneo hyperbolic heat conduction model (see Fig. 1) and the dispersion curves corresponding to Lord–Shulman thermoelasticity (see
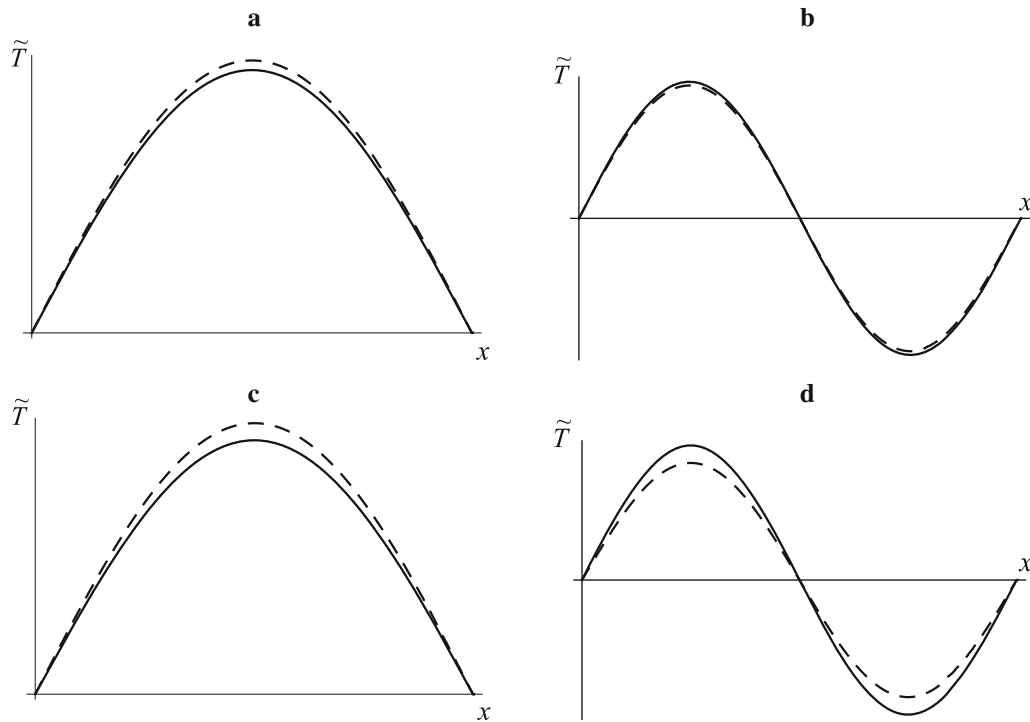
Fig. 9 The comparison of the temperature profiles

Figs. 5, 6), as well as the comparison of the dynamic problem solutions (see Fig. 9), allows us to conclude that in many cases the mutual influence of the thermal and mechanical processes is not very important for description of the heat conduction process. Hence, the mechanical processes can be ignored when the heat flux relaxation time will be determined by the method suggested above.

4 Hyperbolic thermoviscoelasticity

4.1 A statement of the coupled problem of hyperbolic thermoviscoelasticity

An original approach to derivation of a hyperbolic theory of thermoviscoelasticity is suggested in [44]. Neither the hypothesis of fading memory nor the rheological models are used to construct this theory. The approach that is developed in [44] (see also [41–43]) is based on the idea of using the purely mechanical model of a continuum with internal rotational degrees of freedom (a one-rotor gyrostat continuum) in order to describe behavior of the ordinary material medium (medium without internal degrees of freedom) possessing not only mechanical properties but also the thermal ones. In the context of this model, the original treatment of physical nature of the mechanism of thermal conduction and internal damping is considered. The volume and shear viscosities introduced in the context of the model differ from the analogous quantities used in the known theories. In [44], the volume and shear viscosities are determined by using experimental values of the acoustic wave attenuation factor.

The summary of the basic equations of the coupled problem of thermoviscoelasticity suggested [44] is

$$\nabla \cdot \tilde{\boldsymbol{\tau}}^s - \nabla \times \tilde{\mathbf{q}} + \rho \mathbf{f} = \rho \frac{d^2 \mathbf{u}}{dt^2}, \quad \nabla \times \tilde{\boldsymbol{\mu}}_v = 2\tilde{\mathbf{q}}, \quad \nabla \times \boldsymbol{\varphi} = \mathbf{0},$$

$$\tilde{\boldsymbol{\tau}}^s = \left[\left(K - \frac{2}{3} G \right) \varepsilon - \alpha_* K \tilde{T} + p \right] \mathbf{E} + 2 G \, \boldsymbol{\varepsilon}^s, \quad \boldsymbol{\varepsilon}^s = \frac{1}{2} \left(\nabla \mathbf{u} + \nabla \mathbf{u}^T \right),$$

$$\tilde{q} = \frac{(\eta_q - \eta_s) \lambda \alpha_*^2 K^2 T_*}{\rho c_v^2 \eta_v^2} \, \boldsymbol{\gamma} - \frac{\alpha_* K T_* \eta_s}{\rho c_v \eta_v} \, \boldsymbol{\psi} + \mathbf{t}, \quad \boldsymbol{\gamma} = \nabla \times \mathbf{u} - 2\boldsymbol{\varphi},$$

$$\Delta p = \frac{\tau\alpha_*K}{\eta_v}\left[\rho\frac{d^2\tilde{T}}{dt^2} + \frac{\alpha_*KT_*}{c_v}\frac{d^2\varepsilon}{dt^2}\right], \quad \Delta\mathbf{t} = \frac{\tau\alpha_*KT_*}{c_v\eta_v}\frac{d^2\boldsymbol{\psi}}{dt^2}, \quad \varepsilon = \mathrm{tr}\,\boldsymbol{\varepsilon}^s,$$

$$\Delta\tilde{T} - \frac{\rho c_v}{\lambda}\left[\frac{d\tilde{T}}{dt} + \tau\frac{d^2\tilde{T}}{dt^2}\right] = \alpha_*KT_*\left(\frac{1}{\lambda} - \frac{1}{c_v\eta_v}\right)\left[\frac{d\varepsilon}{dt} + \tau\frac{d^2\varepsilon}{dt^2}\right] - \rho\nabla\cdot\mathbf{L}_h,$$

$$(\eta_q - \eta_s)\Delta\boldsymbol{\psi} - \rho\left(\frac{d\boldsymbol{\psi}}{dt} + \tau\frac{d^2\boldsymbol{\psi}}{dt^2}\right) =$$

$$= \frac{\lambda\alpha_*K}{c_v\eta_v}\left[\eta_s\,\Delta\nabla\times\mathbf{u} - \rho\left(\frac{d\nabla\times\mathbf{u}}{dt} + \tau\frac{d^2\nabla\times\mathbf{u}}{dt^2}\right)\right] - \frac{\lambda\,\rho^2}{T_*}\nabla\times\mathbf{L}_h. \tag{49}$$

Here $\tilde{\boldsymbol{\tau}}^s = \boldsymbol{\tau}^s + p\,\mathbf{E}$ is the symmetrical stress tensor, $\tilde{\mathbf{q}} = \mathbf{q} + \mathbf{t}$ is the stress vector characterizing the antisymmetric part of the stress tensor, the $\tilde{\boldsymbol{\mu}}_v$ is the moment stress vector characterizing the antisymmetric part of the moment stress tensor, $\boldsymbol{\varphi}$ is the rotation vector. The quantity $\nabla\cdot\mathbf{L}_h$ characterizes the heat supply per unit mass, and the quantity $\nabla\times\mathbf{L}_h$ characterizes an external influence of different non-mechanical nature. The system of differential Eq. (49) contains three specific parameters of the model: η_v is the characteristic of the volume (acoustic) viscosity, and η_s and η_q are the characteristics of the shear viscosity. The first and second equations in (49) are the equations of motion. The third equations in (49) are the kinematic restriction. The quantities p and $\mathbf{t}$ are considered to be thermodynamic stresses. The constitutive equations for p and $\mathbf{t}$ are represented by the differential equations, namely the eighth and ninth equations in (49). The vector quantity $\boldsymbol{\psi}$ describes an influence of viscous properties of a substance on vector $\mathbf{q}$ characterizing the antisymmetric part of the stress tensor. The eleventh equation in (49) is the heat conduction equation. The twelfth one is an auxiliary equation which is necessary to determine vector $\boldsymbol{\psi}$ and vector $\mathbf{t}$ which is determined by the differential equation containing vector $\boldsymbol{\psi}$ on the right-hand side. It is easy to see that the thermodynamic stresses p and $\mathbf{t}$ vanish when $\eta_v \to \infty$. In this case, the problem of thermoviscoelasticity turns into the hyperbolic type problem of thermoelasticity.

The method of determination of the volume (acoustic) viscosity η_v, applied in [44], is based on using experimental values of the longitudinal wave velocity and the longitudinal wave attenuation factor as well as the value of the heat flux relaxation time that follows from the assumption that the velocity of thermal wave propagation is equal to the theoretical value of the sound velocity. It is important to note that if we decline this assumption and replace the value of τ by some other value, then we obtain the values of volume (acoustic) viscosity η_v different from the values presented in [44]. The method of determination of the shear viscosities η_s and η_q, applied in [44], is based on using experimental values of the transverse wave velocity and the transverse wave attenuation factor as well as the approximate formula according to which the difference $\eta_q - \eta_q$ is proportional to the heat flux relaxation time. Thus, if we replace the aforesaid value of τ by some other value, then we obtain the values of shear viscosities η_s and η_q different from the values presented in [44].

4.2 The problems of longitudinal and transverse wave propagation in the hyperbolic thermoviscoelasticity

As shown in [44], from Eq. (49) it follows that the longitudinal wave propagation is described by the system of equations

$$\Delta T + \rho\nabla\cdot\mathbf{L}_h = \frac{\rho c_v}{\lambda}\left(\frac{\partial T}{\partial t} + \tau\frac{\partial^2 T}{\partial t^2}\right) + \frac{\alpha_*KT_*}{\lambda}\left(1 - \frac{\lambda}{c_v\eta_v}\right)\left(\frac{\partial\varepsilon}{\partial t} + \tau\frac{\partial^2\varepsilon}{\partial t^2}\right), \tag{50}$$

$$\left(K + \frac{4}{3}G\right)\Delta\varepsilon - \alpha_*K\Delta T + \rho\nabla\cdot\mathbf{f} = \left(\rho - \frac{\tau\alpha_*^2K^2T_*}{c_v\eta_v}\right)\frac{\partial^2\varepsilon}{\partial t^2} - \frac{\rho\tau\alpha_*K}{\eta_v}\frac{\partial^2 T}{\partial t^2}, \tag{51}$$

and the transverse wave propagation is described by the system of equations

$$\Delta\boldsymbol{\psi} - \frac{\eta_s\lambda\alpha_*K}{c_v\eta_v(\eta_q - \eta_s)}\Delta\boldsymbol{\phi} + \frac{\lambda\,\rho^2}{T_*(\eta_q - \eta_s)}\nabla\times\mathbf{L}_h =$$

$$= \frac{\rho}{\eta_q - \eta_s}\left(\frac{\partial\boldsymbol{\psi}}{\partial t} + \tau\frac{\partial^2\boldsymbol{\psi}}{\partial t^2}\right) - \frac{\rho\lambda\alpha_*K}{c_v\eta_v(\eta_q - \eta_s)}\left(\frac{\partial\boldsymbol{\phi}}{\partial t} + \tau\frac{\partial^2\boldsymbol{\phi}}{\partial t^2}\right), \tag{52}$$

$$\left(G + \frac{(\eta_q - \eta_s)\lambda\alpha_*^2 K^2 T_*}{\rho c_v^2 \eta_v^2} \right) \Delta\boldsymbol{\phi} - \frac{\eta_s \alpha_* K T_*}{\rho c_v \eta_v} \Delta\boldsymbol{\psi} + \rho \nabla \times \mathbf{f} =$$

$$= \rho \frac{\partial^2 \boldsymbol{\phi}}{\partial t^2} - \frac{\tau \alpha_* K T_*}{c_v \eta_v} \frac{\partial^2 \boldsymbol{\psi}}{\partial t^2} , \tag{53}$$

where the notation $\boldsymbol{\phi} = \nabla \times \mathbf{u}$ is used. Thus, in the considered theory of thermoviscoelasticity, the system of differential equations describing the longitudinal waves and the system of differential equations describing the transverse waves are independent of each other. The heat conduction Eq. (50) in the problem of longitudinal wave propagation, as well as the heat conduction equation in the Lord–Shulman theory, contains the second time derivatives of the temperature and the volume strain. Such terms are absent in the classical heat conduction equation. If $\tau = 0$, then these terms vanish in Eq. (50). However, even in this case, the heat conduction Eq. (50) differs from the classical one since the coefficient of the volume strain in Eq. (50) depends on the volume viscosity, whereas in the classical heat conduction equation it does not depend on this parameter. The equation of motion (51) in the problem of longitudinal wave propagation contains the second time derivative of the temperature. Such term is absent in the classical equation of motion. Equation (52) in the problem of transverse wave propagation has the same structure as the heat conduction Eq. (50) in the problem of longitudinal wave propagation. The only difference is the fact that Eq. (52) contains both the Laplacian of function $\boldsymbol{\psi}$ and the Laplacian of function $\boldsymbol{\phi}$, whereas the heat conduction Eq. (50) contains only the Laplacian of temperature and does not contain the Laplacian of the volume strain. The equation of motion (53) in the problem of transverse wave propagation contains several additional terms compared with the classical equation, and it passes into the classical equation when the parameters η_s, η_q and τ become equal to zero.

4.3 Dispersion relations in the coupled problem of thermoviscoelasticity

In order to analyze the dispersion relations, we consider two one-dimensional problems of wave propagation in the direction of x-coordinate. The first one is the problem of longitudinal wave propagation. The second one is the problem of transverse wave propagation. Further, external influences of all sorts are assumed to be equal to zero.

The problem of longitudinal wave propagation. It is not difficult to show that Eqs. (50), (51) describing the longitudinal wave propagation can be reduced to the following equation in variable ε (or to the same equation in variable T):

$$\frac{\partial^4 \varepsilon}{\partial x^4} - (A_1 + A_2)\frac{\partial^4 \varepsilon}{\partial t^2 \partial x^2} - A_3\frac{\partial^3 \varepsilon}{\partial t \partial x^2} +$$

$$+ A_1 A_3 (1 - A_4)\frac{\partial^3 \varepsilon}{\partial t^3} + A_1 A_2 (1 - A_4)\frac{\partial^4 \varepsilon}{\partial t^4} = 0,$$

$$A_1 = \frac{\rho}{K + \frac{4}{3}G}\left(1 - \frac{\tau \alpha_*^2 K^2 T_*}{\rho c_v \eta_v} \right), \quad A_2 = \tau A_3,$$

$$A_3 = \frac{\rho c_v}{\lambda} + \frac{\alpha_*^2 K T_*}{\lambda(1 + \frac{4}{3}GK^{-1})}\left(1 - \frac{\lambda}{c_v \eta_v} \right),$$

$$A_4 = \frac{\alpha_*^2 K^2 T_*[1 - \lambda/(c_v \eta_v)]\left(\rho c_v \eta_v - \tau\alpha_*^2 K^2 T_* - \tau\rho c_v[K + \frac{4}{3}G]\right)}{\left(\rho c_v[K + \frac{4}{3}G] + \alpha_*^2 K^2 T_*[1 - \lambda/(c_v \eta_v)]\right)\left(\rho c_v \eta_v - \tau\alpha_*^2 K^2 T_*\right)}. \tag{54}$$

It is easy to see that the first equation in Eq. (54) coincides with Eq. (30) of the Lord–Shulman theory. However, the constants A_i in Eq. (54) differ from the corresponding constants given by Eq. (31). At the same time, when $\eta_v \to \infty$, the constants A_i in Eq. (54) turn into the constants A_i given by Eq. (31). When $\tau \to 0$, from Eq. (54) it follows

$$\frac{\partial^4 \varepsilon}{\partial x^4} - A_1\frac{\partial^4 \varepsilon}{\partial t^2 \partial x^2} - A_3\frac{\partial^3 \varepsilon}{\partial t \partial x^2} + A_1 A_3(1 - A_4)\frac{\partial^3 \varepsilon}{\partial t^3} = 0.$$

$$A_1 = \frac{\rho}{K + \frac{4}{3}G}, \quad A_3 = \frac{\rho c_v}{\lambda} + \frac{\alpha_*^2 K T_*}{\lambda(1 + \frac{4}{3}GK^{-1})}\left(1 - \frac{\lambda}{c_v \eta_v} \right),$$
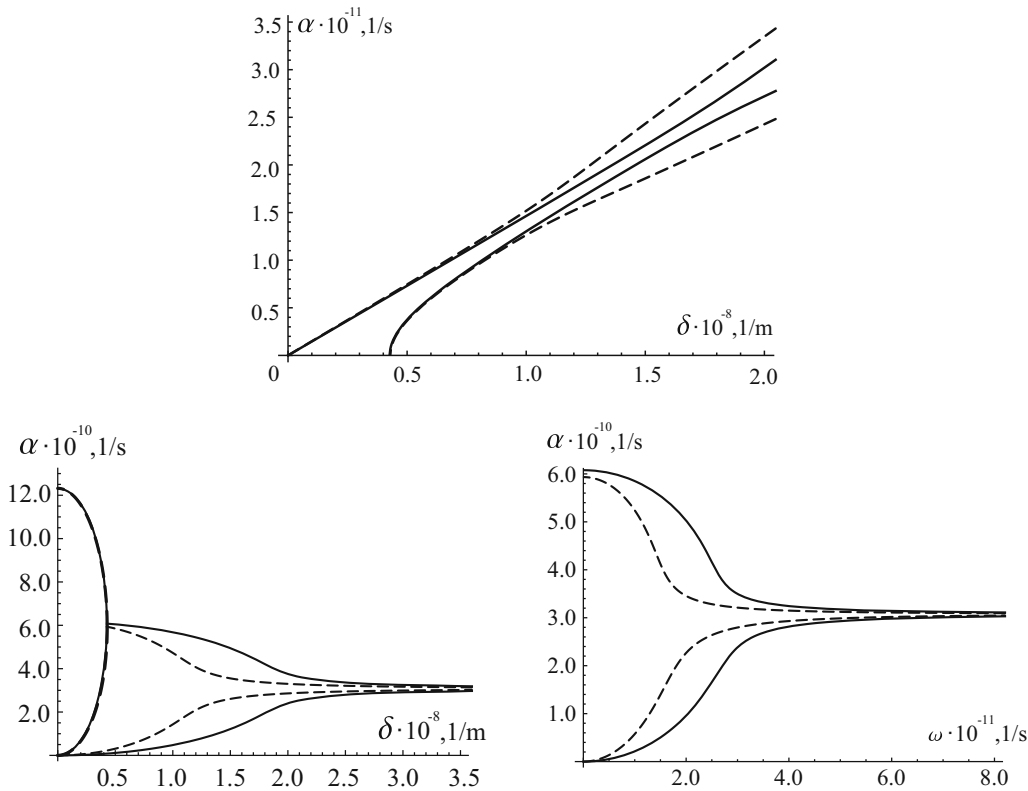
Fig. 10 Dispersion curves for longitudinal waves. The curves shown by *solid lines* correspond to the theory of thermoviscoelasticity. The curves shown by *dashed lines* correspond to the Lord–Shulman theory.

$$A_4 = \frac{\alpha_*^2 K^2 T_* [1 - \lambda/(c_v \eta_v)]}{\rho c_v [K + \frac{4}{3} G] + \alpha_*^2 K^2 T_* [1 - \lambda/(c_v \eta_v)]}. \tag{55}$$

It is important to note that the first equation in Eq. (55) coincides with Eq. (32) of the classical theory of thermoelasticity, but the constants A_1, A_3, A_4 given by Eq. (55) coincide with the corresponding constants of the classical theory only when $\eta_v \to \infty$.

Since the first equation in Eq. (54) is the same as the corresponding equation of the Lord–Shulman theory, all the qualitative results obtained for the coupled problem of thermoelasticity, namely the formulas approximating the dispersion curves and the equations for the asymptotes of the dispersion curves, remain valid in the case of the considered theory of thermoviscoelasticity. Figure 10 illustrates the quantitative difference between the dispersion curves corresponding to Eq. (54) and the dispersion curves corresponding to the Lord–Shulman theory. The dispersion curves shown in Fig. 10 are obtained for the real physical parameters of mercury. The values of τ and η_v are taken from [44]. As seen from Fig. 10, the acoustic and thermal curves have the common asymptotes. This is due to the fact that the value of τ is chosen based on the assumption that the velocity of thermal wave propagation is equal to the theoretical value of the sound velocity. If we abandoned this assumption, the dispersion curves would look like the dispersion curves in Figs. 5, 6.

The problem of transverse wave propagation. It is not difficult to show that Eqs. (52), (53) describing the transverse wave propagation can be reduced to the following equation in variable $\boldsymbol{\phi}$:

$$\frac{\partial^4 \boldsymbol{\phi}}{\partial x^4} - (A_1 + A_2) \frac{\partial^4 \boldsymbol{\phi}}{\partial t^2 \partial x^2} - A_3 \frac{\partial^3 \boldsymbol{\phi}}{\partial t \partial x^2} +$$
$$+ A_1 A_3 (1 - A_4) \frac{\partial^3 \boldsymbol{\phi}}{\partial t^3} + A_1 A_2 (1 - A_4) \frac{\partial^4 \boldsymbol{\phi}}{\partial t^4} = \boldsymbol{0},$$
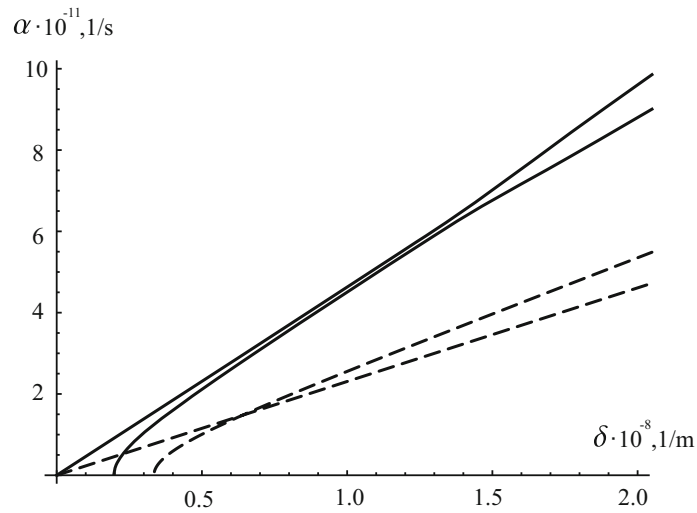
Fig. 11 The wavenumber dependences of the frequency. *The solid lines* correspond to longitudinal waves. *The dashed lines* correspond to transverse waves

$$A_1 = \frac{\rho \left[\rho c_v^2 \eta_v^2 (\eta_q - \eta_s) - \tau \lambda \alpha_*^2 K^2 T_* \eta_s \right]}{G \rho c_v^2 \eta_v^2 (\eta_q - \eta_s) + \lambda \alpha_*^2 K^2 T_* \eta_q (\eta_q - 2\eta_s)}, \quad A_2 = \tau A_3,$$

$$A_3 = \frac{\rho \left[G \rho c_v^2 \eta_v^2 + \lambda \alpha_*^2 K^2 T_* (\eta_q - 2\eta_s) \right]}{G \rho c_v^2 \eta_v^2 (\eta_q - \eta_s) + \lambda \alpha_*^2 K^2 T_* \eta_q (\eta_q - 2\eta_s)},$$

$$A_4 = \frac{\lambda \alpha_*^2 K^2 T_* (\eta_q - 2\eta_s) \left[\rho c_v^2 \eta_v^2 (\tau G - \eta_s) + \tau \lambda \alpha_*^2 K^2 T_* (\eta_q - \eta_s) \right]}{\left(\rho c_v^2 \eta_v^2 [\eta_q - \eta_s] - \tau \lambda \alpha_*^2 K^2 T_* \eta_s \right) \left(G \rho c_v^2 \eta_v^2 + \lambda \alpha_*^2 K^2 T_* [\eta_q - 2\eta_s] \right)}. \tag{56}$$

It is easy to see that the first equation in Eq. (56) looks like the first equation in Eq. (54). The only difference is the physical meaning and numerical values of the constants A_i. Therefore, the considered theory of thermoviscoelasticity contains two frequency spectra corresponding to transverse waves. One of them starts from the point zero, and another one possesses the cut-off wavenumber—see Fig. 11, dashed lines. The first spectrum is the acoustic spectrum, and the physical meaning of the second one is not clear now. The behavior of dispersion curves in the case of transverse waves is the same as the behavior of corresponding dispersion curves in the case of longitudinal waves. Figures 11, 12 illustrate the quantitative difference between the dispersion curves for longitudinal waves and the dispersion curves for transverse waves. The dispersion curves shown in Figs. 11, 12 are obtained for the real physical parameters of copper. The values of τ, η_v, η_s and η_q are taken from [44]. As seen from Fig. 12, for the given parameters, the attenuation factor for transverse acoustic waves is much smaller than the attenuation factor for longitudinal acoustic waves, at least at high frequencies.

5 Conclusion

In the presented study, the dispersion relations for the Maxwell–Cattaneo hyperbolic heat conduction equation, the Lord–Shulman theory of thermoelasticity and the theory of thermoviscoelasticity formulated in [44] have been analyzed. In the case of the Lord–Shulman model, the simple formulas that quite accurately approximate the dispersion curves have been obtained. It has been shown that these formulas are valid in the case of the model of thermoviscoelasticity suggested in [44]. Based on the fact that oscillations appear in the decreasing solution of the heat conduction problem when the layer thickness becomes smaller, the experimental method of determination of the heat flux relaxation time has been suggested. By comparison of thermal oscillations obtained as a result of solving the heat conduction problem and the thermoelasticity problem, it has been shown that mechanical processes will not have a considerable influence on the accuracy of the experimental determination of the heat flux relaxation time.
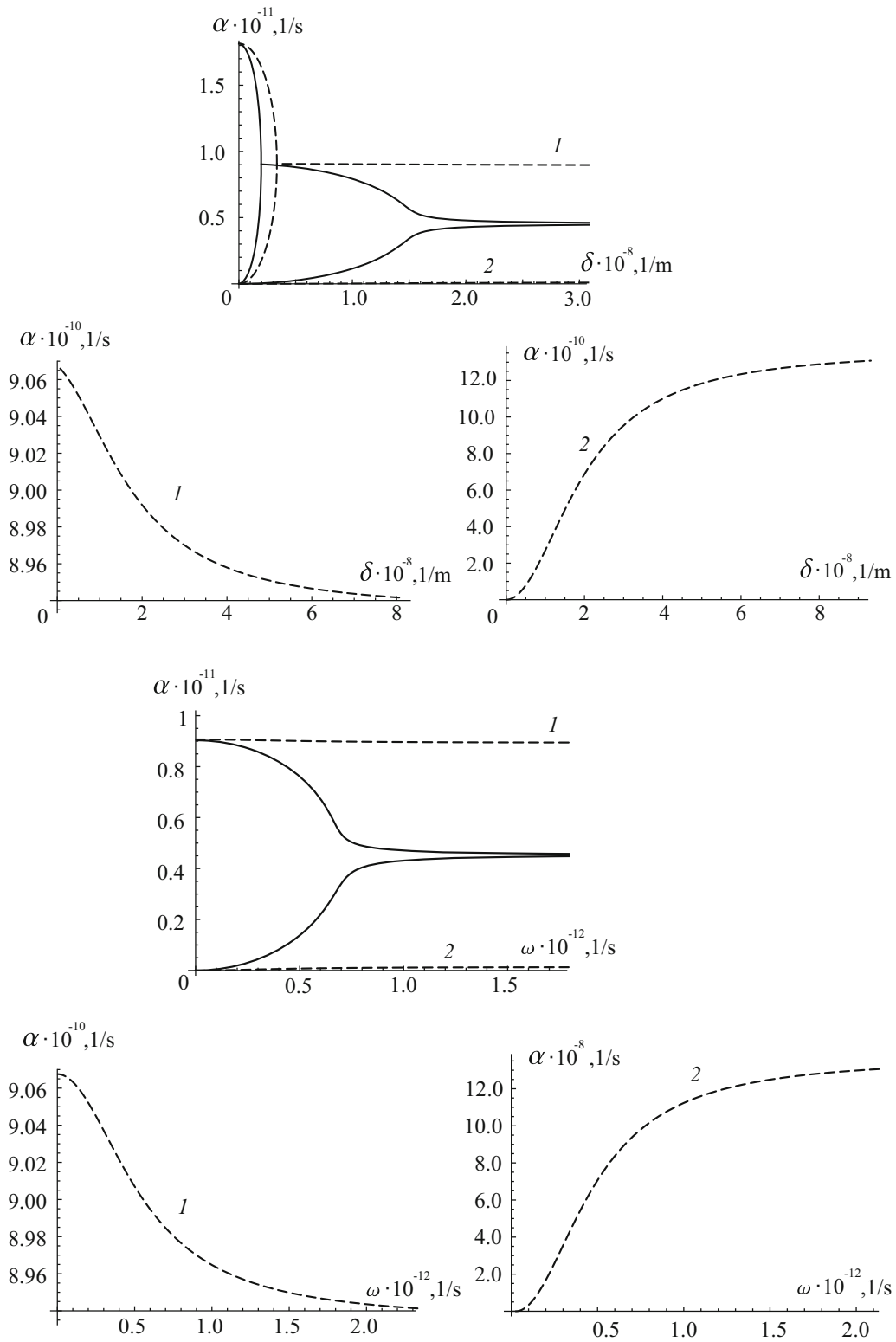
Fig. 12 The wavenumber and frequency dependences of the attenuation factor. The curves shown by *solid lines* correspond to the longitudinal waves. The curves shown by *dashed lines* correspond to the transverse waves

References

1. Pop, E., Sinha, S., Kenneth, E.: Goodson heat generation and transport in nanometer-scale transistors. Proc. IEEE **94**(8), 1587–1601 (2006)
2. Jou, D., Casas-Vazquez, J., Lebon, G.: Extended Irreversible Thermodynamics. Springer, Berlin (1996)
3. Chandrasekharaiah, D.S.: Hyperbolic thermoelasticity: a review of recent literature. Appl. Mech. Rev. **51**, 705–729 (1998)
4. Tzou, D.Y.: Macro-to-Microscale Heat Transfer. The Lagging Behaviour. Taylor and Francis, New York (1997)
5. Shashkov, A. G., Bubnov, V. A., Yanovski, S. Y.: Wave phenomena of heat conductivity: system and structural approach. (1993).(in Russian)
6. Wang, C.C.: The principle of fading memory. Arch. Ration. Mech. Anal. **18**(5), 343–366 (1965)
7. Tzou, D.Y.: On the thermal shock wave induced by a moving heat source. Int. J. Heat Mass Transf. **111**, 232–238 (1989)
8. Qiu, T.Q., Tien, C.L.: Short-pulse laser heating on metals. Int. J. Heat Mass Transf. **35**(3), 719–726 (1992)
9. Sobolev, S.L.: Transport processes and traveling waves in systems with local nonequilibrium. Sov. Phys. Uspekhi **34**(3), 217 (1991)
10. Cattaneo, C.: A form of heat conduction equation which eliminates the paradox of instantaneous propagation. Compte Rendus **247**, 431–433 (1958)
11. Vernotte, P.: Les paradoxes de la theorie continue de lequation de la chaleur. CR Acad. Sci. **246**(22), 3154–3155 (1958)
12. Lykov, A. V.: Theory of heat conduction. Vysshaya Shkola, Moscow. (1967): 599. (in russian)
13. Babenkov, M.B., Ivanova, E.A.: Analysis of the wave propagation processes in heat transfer problems of the hyperbolic type. Contin. Mech. Thermodyn. **26**(4), 483–502 (2014). doi:10.1007/s00161-013-0315-8
14. Peshkov, V.: Second sound in helium II. J. Phys. **8**, 381 (1944)
15. Liu, Y., Mandelis, A.: Laser optical and photothermal thermometry of solids and thin films. Exp. Methods Phys. Sci. **42**, 297–336 (2009)
16. Magunov, A.N.: Laser thermometry of solids: state of the art and problems. Meas. Tech. **45**(2), 173–181 (2002)
17. Magunov, A.N.: Laser Thermometry of Solids. Cambridge International Science Publishing, Cambridge (2003)
18. Wang, X.: Experimental Micro/nanoscale Thermal Transport. Wiley, Hoboken (2012)
19. Krilovich, V.I., Bil, G.N., Ivakin, E.V., Rubanov, A.C.: Experimental determination heat velocity. NASB **1**, 129–134 (2000). (in Russian)
20. Ivakin, E.V., Kizak, A.I., Rubanov, A.S.: Active spectroscopy of rayleigh light-scattering in study of heat-transfer. Izvestiya Akademii Nauk SSSR Seriya fizicheskaya **56**(12), 130–134 (1992). (in Russian)
21. Ivakin, E.V., Lazaruk, A.M., Filipov, V.V.: Application of laser induced gratings for thermal diffusivity measurements of solids. Proc. SPIE **2648**, 196–206 (1995). (in Russian)
22. Xu, F., Tianjian, Lu: Introduction to Skin Biothermomechanics and Thermal Pain, vol. 7. Science Press, New York (2011)
23. Grassmann, A., Peters, F.: Experimental investigation of heat conduction in wet sand. Heat Mass Transf. **35**(4), 289–294 (1999)
24. Herwig, H., Beckert, K.: Experimental evidence about the controversy concerning Fourier or non-Fourier heat conduction in materials with a nonhomogeneous inner structure. Heat Mass Transf. **36**(5), 387–392 (2000)
25. Kaminski, W.: Hyperbolic heat conduction equation for materials with a nonhomogeneous inner structure. J. Heat Transf. **112**(3), 555–560 (1990)
26. Mitra, K., Kumar, S., Vedavarz, A., Moallemi, M.K.: Experimental evidence of hyperbolic heat conduction in processed meat. J. Heat Transf. **117**, 568–573 (1995)
27. Roetzel, W., Putra, N., Das, Sarit K.: Experiment and analysis for non-Fourier conduction in materials with non-homogeneous inner structure. Int. J. Therm. Sci. **42**, 541–552 (2003)
28. Vovnenko, N.V., Zimin, B.A., Sud'enkov, YuV: Nonequilibrium motion of a metal surface exposed to sub-microsecond laser pulses. Zhurnal tekhnicheskoi fiziki **80**(7), 41–45 (2010). (in Russian)
29. Sudenkov, Y.V., Pavlishin, A.I.: Nanosecond pressure pulses propagating at anomalously high velocities in metal foils. Tech. Phys. Lett. **29**(6), 491–493 (2003)
30. Szekeres, A., Fekete, B.: Continuummechanics-heat conduction-cognition. Period. Polytech. Eng. Mech. Eng. **59**(1), 8 (2015)
31. Tzou, D.Y.: An engineering assessment to the relaxation time in thermal wave propagation. Int. J. Heat Mass Transf. **36**(7), 1845–1851 (1993). doi:10.1016/s0017-9310(05)80171-1
32. Gembarovic, J., Majernik, V.: Non-Fourier propagation of heat pulses in finite medium. Int. J. Heat Mass Transf. **31**(5), 1073–1080 (1988)
33. Poletkin, K.V., Gurzadyan, G.G., Shang, J., Kulish, V.: Ultrafast heat transfer on nanoscale in thin gold films. Appl. Phys. B **107**, 137–143 (2012)
34. Sieniutycz, S.: The variational principles of classical type for non-coupled non-stationary irreversible transport processes with convective motion and relaxation, S. Sieniutycz. Int. J. Heat Mass Transf. **20**(11), 1221–1231 (1977)
35. Majumdar, A.: Microscale heat conduction in lelectnc thin films. J. Heat Transf. **115**, 7 (1993)
36. Matsunaga, R. H., dos Santos, I.: Measurement of the thermal relaxation time in agar-gelled water. In: Engineering in Medicine and Biology Society (EMBC), 2012 Annual International Conference of the IEEE. IEEE, pp. 5722–5725 (2012)
37. Lord, H., Shulman, Y.: A generalized dynamical theory of thermoelasticity. J. Mech. Phys. Solids **15**, 299–309 (1967)
38. Green, A.E., Lindsay, K.A.: Thermoelasticity. J. Elast. **2**, 1–7 (1972)
39. Hetnarski, R.B., Ignaczak, J.: Solution-like waves in a low-temperature nonlinear thermoelastic solid. Int. J. Eng. Sci. **34**, 1767–1787 (1996)
40. Green, A.E., Nagdi, P.M.: Thermoelasticity without energy dissipation. J. Elast. **31**, 189–208 (1993)
41. Ivanova, E.A.: Derivation of theory of thermoviscoelasticity by means of two-component medium. Acta Mech. **215**(1–4), 261–286 (2010)
42. Ivanova, E.A.: On one model of generalised continuum and its thermodynamical interpretation. In: Altenbach, H., Maugin, G.A., Erofeev, V. (eds.) Mechanics of Generalized Continua, pp. 151–174. Springer, Berlin (2011)

43. Ivanova, E.A.: Derivation of theory of thermoviscoelasticity by means of two-component Cosserat continuum. Tech. Mech. **32**(2–5), 273–286 (2012)
44. Ivanova, E.A.: Description of mechanism of thermal conduction and internal damping by means of two component Cosserat continuum. Acta Mech. **225**(3), 757–795 (2014)
45. Niu, T., Dai, W.: A hyperbolic two-step model-based finite-difference method for studying thermal deformation in a 3-D thin film exposed to ultrashort pulsed lasers. Numer. Heat Transf. Part A Appl. **53**(12), 1294–1320 (2008)
46. Qin, Y.: Nonlinear Parabolic-Hyperbolic Coupled Systems and Their Attractors, vol. 184. Springer, Berlin (2008)
47. Mondal, S., Mallik, S. H., Kanoria, M.: Fractional order two–temperature dual–phase–lag thermoelasticity with variable thermal conductivity. Int. Sch. Res. Not. vol. 2014, Article ID 646049, 13 pages, (2014). doi:10.1155/2014/646049
48. Babenkov, M.B.: Analysis of dispersion relations of a coupled thermoelasticity problem with regard to heat flux relaxation. J. Appl. Mech, Tech. Phys. **52**(6), 941–949 (2011)
49. Babenkov, M.B.: Propagation of harmonic perturbations in a thermoelastic medium with heat relaxation. J. Appl. Mech. Tech. Phys. **54**(2), 277–286 (2013)
50. Nowacki, W.: Dyn. Probl. Thermoelast. Springer, Berlin (1975)